

2008 ANALOGUE-NUMERICAL MODEL COMPARISONS

Susanne Buiter¹ and Guido Schreurs²

¹ Center for Geodynamics, Geological Survey of Norway, Trondheim; susanne.buiter(at)ngu.no

² Institute of Geological Sciences, University of Bern, Switzerland; schreurs(at)geo.unibe.ch

1 Introduction

We aim to compare results of analogue and numerical models for three experiments in order to constrain and quantify the variability between analogue and numerical models and improve our understanding of causes of differences between analogue and numerical models. This document describes the set-up of the experiments. Please **follow the instructions exactly** and contact the organisers before making any changes in the set-up. Useful comparisons can only be made when all experiments follow the same recipe!

This document replaces the original recipe of January 2008 and is mainly updating the numerical description.

The experiments should be quantified and submitted to us by **28th February 2009**.

Contacts:

Analogue experiments:	Guido Schreurs, schreurs(at)geo.unibe.ch
Numerical experiments:	Susanne Buiter, susanne.buiter(at)ngu.no
Analogue materials benchmark:	Matthias Klinkmüller, matthias(at)geo.unibe.ch
PIV measurements:	Christoph Schrank, schrank(at)geology.utoronto.ca

Website: www.geodynamics.no/benchmarks

2 Minimum requirements

We aim to reduce the level of variability among the model set-ups in comparison with the GeoMod2004 experiments. We therefore ask that the description of the experiments **be followed exactly**.

Analogue experiments require the following features:

- Motor-driven (no hand-screw)
- Minimum width 25 cm (measured along strike of mobile wall)
- Alkor foil on all walls and base (if visibility through a sidewall is needed for PIV, please do the experiment first with foil and repeat the experiment without foil).
- Use of the prescribed sand (contact Guido Schreurs for shipment)

Numerical experiments require the following features:

- Brittle material behaviour
- Boundary friction on sidewalls and base

Numerical models may be 2D or 3D. For 3D models, please run each experiment in addition in 2D mode to enable comparisons among all models.

We kindly ask everyone to carefully document their experiments. Templates for this are available from the website or by e-mail from the organisers. Please follow the instructions for model building and quantification exactly. For an objective quantification it is extremely important that documentation of the experiments is provided in numbers and figures. All figures should have a scale. Images should be sent to us in jpg with compression kept at a minimum, animations preferably in gif, but mpeg or quicktime is accepted too (please specify pc or mac).

3 Model materials

The experiments will only use sand. This granular material mainly deforms by shear zone formation, in combination with dilation and probably only limited elastic deformation. The formation of shear bands in sand is a field of study in itself. Upon loading, sand will first show elastic deformation and plastic strain hardening until it fails at peak strength. This failure is associated with the maximum rate of dilation (Lohrmann et al. 2003; Panien et al. 2006). After initial failure a phase of softening takes place until the dynamic stable strength is reached. The dip angle of shear bands in sand with the direction of maximum compression σ_1 has been shown to vary between:

- The Coulomb angle: $45^\circ - \phi/2$
- The Roscoe angle: $45^\circ - \psi/2$ (Roscoe, 1970)
- The Arthur angle: $45^\circ - (\psi + \phi)/4$ (Vardoulakis, 1980)

Here ϕ is the angle of internal friction and ψ the angle of dilation. ϕ defines the ratio between shear stress (τ) and normal stress (σ_n) for zero cohesion (C): $\tau = \tan(\phi)\sigma_n + C$ and can be measured in a ring-shear tester or with a Hubbert-type shear box. ψ is the ratio of the rate of volumetric strain ($\varepsilon_v = \varepsilon_1 + \varepsilon_2 + \varepsilon_3$) and the rate of shear strain γ : $\tan \psi = -(\delta\varepsilon_v)/\delta\gamma$.

Elastic behaviour is characterised by two elastic parameters, Young's modulus E and Poisson's ratio ν or the Lamé parameters λ and G . G is also called the shear modulus. Young's modulus is the ratio of uniaxial stress and strain: $E = \sigma_1/\varepsilon_1$. Poisson's ratio is the negative ratio of transverse strain to longitudinal strain under condition of uniaxial stress: $\nu = -\varepsilon_2/\varepsilon_1 = -\varepsilon_3/\varepsilon_1$. From E and ν , the values for λ and G can be derived and vice versa (Turcotte and Schubert, 2002; Jaeger et al. 2007): $E = G(3\lambda + 2G)/(\lambda + G)$ and $\nu = \lambda/(2(\lambda + G))$. A fifth elastic parameter is the bulk modulus K defined by the ratio of mean stress over volumetric strain. K can also be written as $K = (\lambda + 2G/3)$ or $K = E/(3(1-2\nu))$ (and $1/K$ is the bulk compressibility).

For an incompressible material, the dilation (volume change or volumetric strain) is zero and $\varepsilon_1 + \varepsilon_2 + \varepsilon_3 = 0$. Then $1/K = 0$, $K \rightarrow \infty$, $\nu \rightarrow 0.5$, $\lambda \rightarrow \infty$ and $E \rightarrow 3G$.

3.1 Analogue model materials and model building

All laboratories will use **the same two sands**. Experiment 1A uses only quartz sand, whereas both quartz and corundum sand are used in experiments 1B and 2. Please contact Guido Schreurs well in advance to arrange a sand shipment. Specify the dimensions (length x width) of your modelling apparatus, the experiments that are planned and the quantity of each sand that is needed. Please document how the material is stored after you received the sand shipment: room temperature and especially humidity. Please avoid direct sunlight.

The sand should be sieved from 20 cm height with a filling rate of 250 ml/minute using the sieve structure of Fig. 1. Do not use a sieving machine. The experiment should not be pre-compacted.

Sand can be scraped off, please observe the scraping directions given with the experiment descriptions. The scraper should be thin and stiff (Fig. 2).

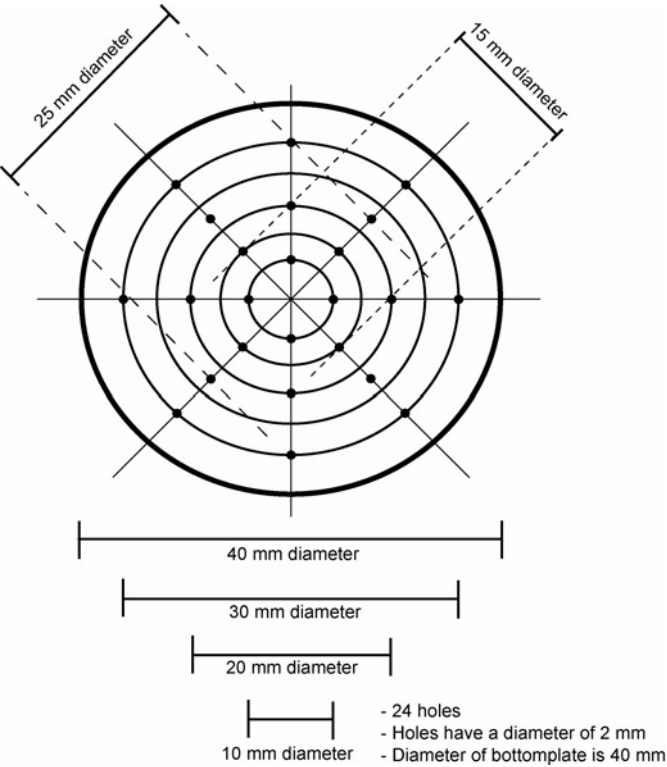


Fig. 1. Sieve structure for sandbox filling.

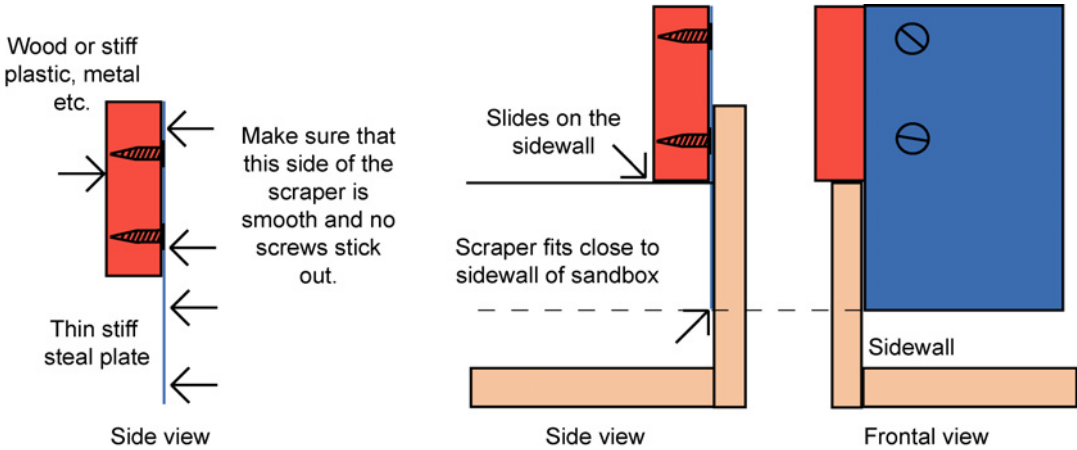


Fig. 2. Scraper to scrape off excess sand (for all analogue experiments).

3.2 Numerical model materials

We expect that there will be differences among the numerical models in constitutive equations. We therefore ask that all numerical models will be run with a minimum set of prescribed material behaviour (Table 1) in order to allow model comparisons among many models. We will then build on these by progressively adding complexity in the rheology. Please use the minimum set for experiments 1A, 1B and 2. Tests with additional rheology components are encouraged for all experiments.

3.2.1 Minimum material description

Parameter	cm-scale	km-scale
Quartz sand		
Density	1560 kg m ⁻³	1560 kg m ⁻³
Angle of internal friction at peak strength	36°	36°
Angle of internal friction at stable strength	31°	31°
Apparent internal cohesion	30 Pa	3 MPa
Boundary friction at peak strength	16°	16°
Boundary friction at stable strength	14°	14°
Apparent boundary cohesion	30 Pa	3 MPa
Dilation angle	0	0
Corundum sand		
Density	1890 kg m ⁻³	1890 kg m ⁻³
Angle of internal friction at peak strength	36°	36°
Angle of internal friction at stable strength	31°	31°
Apparent internal cohesion	30 Pa	3 MPa
Boundary friction at peak strength	24°	24°
Boundary friction at stable strength	23°	23°
Apparent boundary cohesion	30 Pa	3 MPa
Dilation angle	0	0
Background viscosity	10 ¹² Pa s	10 ²⁷ Pa s
Gravitational acceleration	9.81 m s ⁻²	9.81 m s ⁻²
Time step	3.6 s	3.6 x 10 ¹⁰ s

Table 1. Material properties (minimum set) for numerical models

The values for angle of internal friction, cohesion and boundary friction were measured by Matthias Klinkmüller with the ring-shear tester of GFZ Potsdam for 3-5 samples of the same sand. We report rounded average values in Table 1. The peak angle of internal friction varies between 34.4° and 37.0° for quartz sand (5 measurements) and between 35.1° and 36.1° for corundum sand (3 measurements). The boundary friction at peak strength varies between 10.7° and 21.2° for quartz sand on foil (5 measurements) and between 23.4° and 24.9° for corundum sand on foil (3 measurements). The variation in cohesion is typically large and is between 18.9 Pa and 68.8 Pa for quartz sand and between 15.1 Pa and 28.4 Pa for corundum sand. The variation is even larger for apparent boundary cohesion, between 13.6 Pa and 141.3 Pa for quartz sand on foil and between 23.1 and 44.2 for corundum sand on foil. We have severely simplified the cohesion value in our experiments, but 30 Pa is within the measurement range for all materials. Cohesion is the linearly extrapolated value at zero normal stress ($\sigma_n = 0$), called apparent cohesion in Table 1. At low normal stresses, however, the failure envelope is probably no longer a straight line, but instead has a convex-leftward shape with negligible cohesion (Schellart, 2000; Panien et al., 2006). For codes that can model this behaviour, it is encouraged to test the role of zero cohesion at low normal stress by running an additional experiment.

To enable comparison among the different types of codes, we explicitly prescribe the softening behaviour from peak strength to stable strength. Softening is simulated by a linear decrease from the peak angle to the stable angle over a finite strain interval of 0.5 to 1.0. Finite strain is the total accumulated effective strain as measured by the second invariant of the strain tensor. Note that boundary friction also shows softening behaviour.

If the code includes elastic material behaviour by default, please ‘switch it off’ by using a large Young’s modulus of 10^{17} Pa (km-scale) or 10^{12} (cm-scale) and Poisson’s ratio 0.5. This value for Young’s modulus was derived by requiring that the time-scale of our experiments is much larger than the Maxwell relaxation time (which is defined as the ratio of viscosity over shear modulus).

In sandbox-type models an important role is played by the boundaries and the frictional sliding of sand against these boundaries. We ask therefore that boundary friction is explicitly included in the numerical models, though the exact implementation is free. Please describe the method you have used and document its validity by demonstrating that the stable wedge experiment (1A) is indeed stable for the values in Table 1 and becomes unstable if basal friction is decreased to 1° . The boundary friction values show relatively large variations and we encourage tests of the sensitivity of experiments 1B and 2 to variations in boundary friction.

3.2.2 *Dilation*

The peak dilation angle (the dilation angle at peak strength) for the dry sands used in these experiments is difficult to determine with a ring-shear tester. It requires measurements of the changes in volumetric strain, but the volumetric strain depends on the width of the initial shear zone that forms. Assuming an initial shear zone width of about 10 times the average grain size (Panien et al., 2006), we obtain very small dilation angles of less than 2° . Measurements of shear band formation in sand indicate that dilation approaches zero once the shear band has formed. To test the effect of compressibility (for codes that can do this), please run the experiments with dilation angles: a) 2° , b) 5° and c) 10° . These experiments should be run **without** strain softening because we assume that the softening from peak to stable strength is caused by dilation of sand at yield. In addition, analogue measurements indicate that dilation goes towards zero once a shear band has formed. This could be simulated by a strain-dependent dilation.

3.2.3 *Elasticity*

The bulk moduli of the quartz and corundum sands were measured performing loading-unloading cycles (maximum load: 20 kPa) with a uniaxial compression tester at GFZ Potsdam. The values vary depending on the degree of compaction, which increases mainly during the first few loading-unloading cycles. Linear regression analysis of the stress-strain curves (up to a strain of 0.00003) during loading of the first ten cycles suggests a bulk modulus of around 200 MPa for both sands under laboratory conditions. Assuming a Poisson’s ratio ν of about 0.25 results in a Young’s modulus E of 300 MPa (cm-scale), or 3×10^{13} Pa (km-scale). These values are so high, that elastic deformation is expected to be minor in the experiments.

However, numerical models could test the role of elasticity in the experiments by progressively changing the values of the elasticity parameters. Please use a) $E = 5$ MPa (cm-scale) or 5×10^{11} Pa (km-scale), $\nu = 0.25$ (Earth-like values) and b) $E = 200$ MPa (cm-scale) or 2×10^{13} Pa (km-scale), $\nu = 0.25$.

In addition, it could be tested whether elasto-visco-plastic models converge to visco-plastic models for high Young’s modulus and Poisson ratio close to 0.5.

4 Experiments 1A and 1B: Brittle compressional wedges

The theory of contractional brittle wedges is described in many papers (e.g. Dahlen et al. 1984; Dahlen and Suppe, 1988; Davis et al. 1983; Zhao et al. 1986). Wedges in the stable field will

slide stably without internal deformation as long as no new material is accreted. Unstable wedges will deform to achieve their critical taper angle (which is given by the sum of surface and base dip angles). The stability field for sand close to that used at Bern University is illustrated in Fig. 3.

The experiment is divided in two:

- A. A stable wedge.
- B. An unstable wedge.

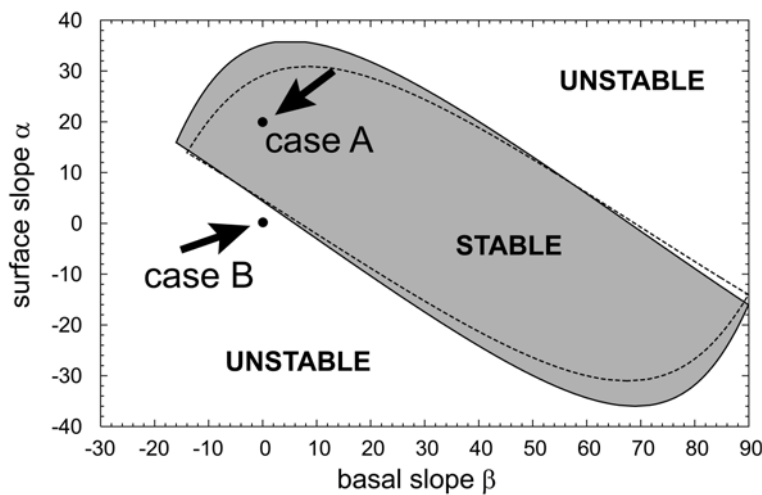


Fig. 3: Stability fields for sand at peak strength (gray field with drawn line) with an angle of internal friction $\phi = 36^\circ$, a cohesion $C = 0$ MPa, basal friction angle $\phi_b = 16^\circ$ and $C_b = 0$ MPa and sand at stable strength (dashed line) with $\phi = 31^\circ$, $C = 0$ MPa, $\phi_b = 14^\circ$ and $C_b = 0$ MPa,

4.1 Experiment 1A: A stable compressional wedge

The aim of this experiment is to verify that the model follows the analytical wedge theory. A brittle wedge with a horizontal base ($\beta = 0^\circ$) and surface slope $\alpha = 20^\circ$ is shortened by inward movement of a mobile wall. The surface slope is in the stable field (Fig. 3) and the wedge should thus slide without internal deformation. The set-up is shown in Fig. 4.

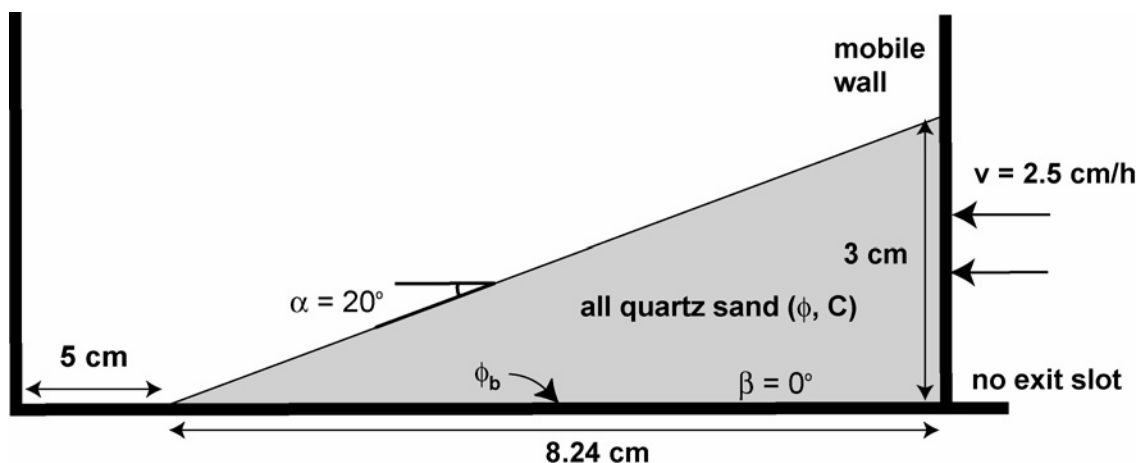


Fig. 4: Set-up of the brittle compressional wedge experiment 1A. All walls and the base are covered with Alkor foil. The wedge is built with quartz sand only.

4.1.1 Analogue model building procedure

This experiment is done with quartz sand only (no layering). The wedge can be built following the instructions in Fig. 5. Make sure that the vertical wall touches the base at all times, so that no sand escapes underneath it. Document the basal domain over which the wall moved by a surface

photo (including the wall) at 4 cm of shortening.

Please see ‘Analogue model materials’ (section 3.1) for additional instructions.

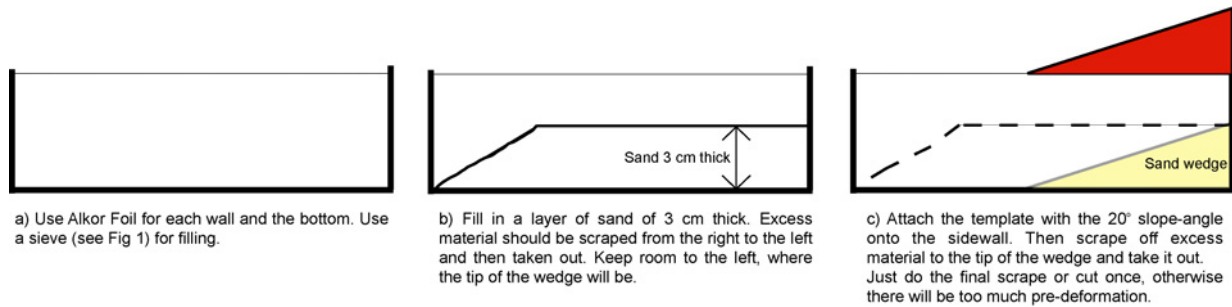


Fig. 5. Procedure for building a wedge in an analogue modelling apparatus.

4.1.2 Numerical model set-up

The experiment can be run at cm or km scale. If scaling up, please use 1 cm = 1 km and 2.5 cm/h = 2.5×10^{-7} m/h (6.94444×10^{-11} m/s). The time step should be 3.6 s (cm-scale) or 3.6×10^{10} s (km-scale).

The building of the mesh may cause problems for numerical models that have quadrilateral elements (triangles or DEM should be easier). In this case, please observe Fig. 6. The resolution of the models should be high enough so that an increasing resolution does not lead to different model results (in this experiment it needs to be shown that the wedge slides without internal deformation). Report the number of solution nodes in the wedge domain and specify if an ‘air’ layer was used.

Some codes may be able to apply the velocity contrast between the mobile wall and the base directly (method 1), however, the GeoMod2004 experiments showed that many codes suffer from numerical problems related to the velocity discontinuity. In that case smooth the velocity discontinuity at the basal corner (marked ‘no exit slot’ in Fig. 4). Linearly decrease the velocity from $v = 2.5$ cm/h over 2 mm to $v = 0$ at the base of the mobile wall (method 2). Please specify which method you have used.

First tests have indicated that some codes are sensitive to the manner in which the velocity is applied: The full velocity can be applied at once or the driving velocity can gradually be build up to reach 2.5 cm/h in a specified number of iterations. Please test whether your results are sensitive to a build-up phase for the driving velocity.

Please see ‘Numerical model materials’ (section 3.2) for additional instructions.

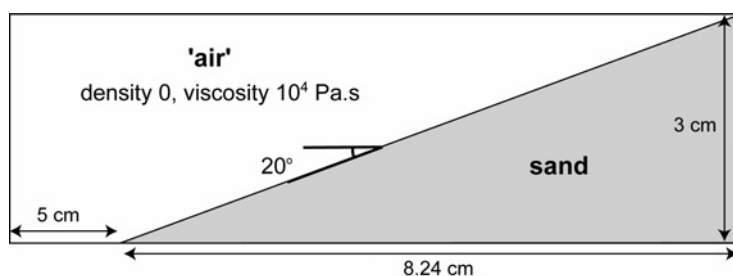


Fig. 6. Numerical models with quadrilateral elements can use an ‘air’ layer (viscosity 10^4 Pas on cm-scale and 10^{19} Pas on km-scale) to obtain a slope of 20° for the sand layer with a regular element

distribution.

4.1.3 Required results

The experiment should be shortened 4 cm. The analogue laboratories need only run this experiment once (unless the results show a deforming wedge!). However, please run an extra experiment if Alkor foil cannot cover the sidewall for visibility for PIV imaging (section 6). Numerical models also need only run this experiment once, but it is encouraged to test the role of resolution for comparison with experiment 1B (provide the values of points 9-12 – see below - at minimum for different resolutions). Please provide the following results:

1. Analogue and numerical models: Cross-sections at the following shortening increments: 0 cm, 0.5, 1.0, 1.5, 2.0, 2.5, 3.0 cm, 3.5, and 4.0 cm. All analogue laboratories should report the cross-sectional evolution as monitored from the side. Laboratories that have access to an X-ray computed tomographer should in addition report the evolution for a cross-section through the middle of the domain (please specify the exact location of the cross-section). Numerical models should show the material field (to enable comparison with the analogue models). 3D numerical models should report the evolution of a cross-section through the middle of the domain (please specify exact location of the cross-section). Please show cross-sectional evolution with ‘mobile wall’ moving from right to left.
2. Analogue and numerical models: An animation of the cross-sectional evolution with each stage indicated.
3. Numerical models: show (1) strain-rate and (2) mean stress (pressure) at the same stages (point 1). Please use the scales (colour and intervals) in Fig. 7.
4. Analogue models and 3D numerical models: Surface views at the same stages (point 1).
5. Analogue models and 3D numerical models: Animation of surface views with stages indicated.
6. Analogue models: Surface photograph at 4.0 cm shortening of the basal domain over which the wall moved (including the wall itself).
7. Analogue models: Please cut experiment at 4.0 cm of shortening and show a section through the middle of the model domain. Please indicate the exact location of the section.
8. Analogue and numerical models: Surface slope at the same stages as give in point 1. Please see Fig. 8 for measurement instructions. Analogue models with access to a scanner should measure a section through the middle of the domain (and report the location of the section). Laboratories that monitor through a glass sidewall can measure at the sidewall (please specify this) and in addition measure surface slope for a section through the middle for 4 cm of shortening.
9. Numerical models: Dissipation of energy at every 0.5 cm (in the wedge domain only):

$$\frac{1}{2} \int_A (\boldsymbol{\sigma} \cdot \dot{\boldsymbol{\varepsilon}}) dA$$

Here A is area for 2D models and volume for 3D models. For 3D models, please provide also the 2D quantity through the middle of the domain (please indicate the exact location of the section).

10. Numerical models: Gravitational rate of work at every 0.5 cm (in the wedge domain only):

$$\int_A (\rho g v_y) dA$$

Here A is area for 2D models and volume for 3D models. For 3D models, please provide also the 2D quantity through the middle of the domain (please indicate the exact location of the section). ρ is density, g gravitational acceleration and v_y the vertical component of velocity.

11. Numerical models: root-mean-square (rms) velocity at every 0.5 cm (in the wedge domain only):

$$v_{rms} = \sqrt{\frac{1}{A} \iint (v_x^2 + v_y^2) dx dy}$$

The integration is over the model domain and A is the area of the model domain. For 3D models, please provide both the 3D value and the 2D quantity through the middle of the domain (please indicate the exact location of the section).

12. Numerical models: Force applied at mobile wall (right hand side boundary) at every 0.5 cm:

$$F = \int_h \sigma_{xx} dz$$

For 3D models, please provide also the 2D quantity through the middle of the domain (please indicate the exact location of the section).

13. Numerical models: Please document: resolution (number of solution nodes, type of element and number of elements horizontally x vertically (if applicable)), ψ , E, ν , whether smoothing is used at the velocity discontinuity, km-scale or cm-scale, whether an air-layer was used.
14. Numerical models: Please show that your stable wedge becomes unstable when the basal boundary friction is reduced to 1° by cross-sections at every 0.5 cm until the first shear zone has formed.

Please show cross-sectional evolution with ‘mobile wall’ moving **from right to the left**.

For numerical modellers: please scale down to the analogue experiments (cm-scale) if necessary. Please use $1 \text{ km} = 1 \text{ cm}$, $10^{-11} \text{ s}^{-1} = 10^{-1} \text{ s}^{-1}$, $1 \text{ MPa} = 10 \text{ Pa}$ and $10^{24} \text{ Pa.s} = 10^9 \text{ Pa.s}$.

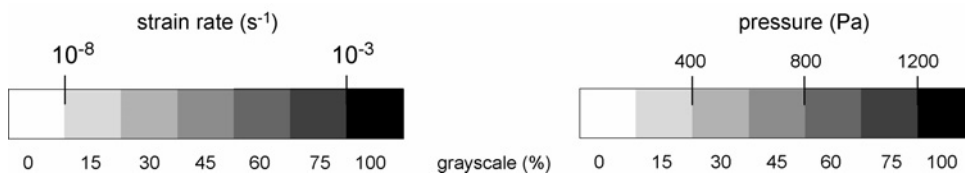


Fig. 7. Scales (colour and magnitude) for numerical strain-rate and pressure plots. Note that these values are for the cm-scale.

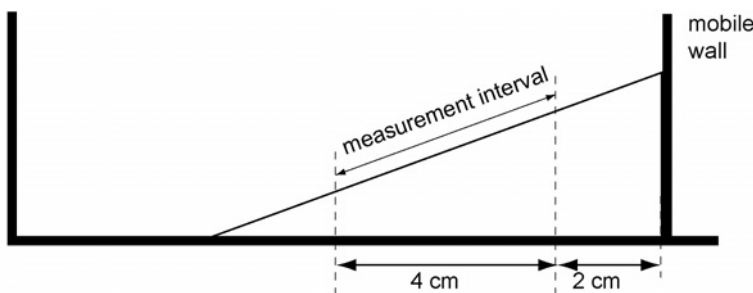


Fig. 8. Measurement of surface slope for experiment 1A.

4.2 Experiment 1B: An unstable compressional wedge

Horizontal layers of sand are shortened by inward movement of a mobile wall (Fig. 9). Both the base and the surface are horizontal ($\alpha = \beta = 0^\circ$) and the ‘wedge’ is thus in the unstable field (Fig. 3). For this case we will compare the thrusts that form and the evolution of surface slope.

4.2.1 Analogue model building procedure

Try to fill in sand as evenly as possible (Fig. 1), in order that each layer only needs to be levelled once! Scrape off the excessive sand (with a thin and very stiff metal plate, Fig. 2) starting at the moving wall and in a direction away from the moving wall. Please make sure that the scraper is parallel to the mobile wall and carefully lower the scraper onto the sand. Make sure that the vertical wall touches the base at all times, so that no sand escapes. Please document the basal domain over which the wall moved by a surface photo (which includes the wall) at 10 cm of shortening.

Please see ‘Analogue model materials’ (section 3.1) for additional instructions.

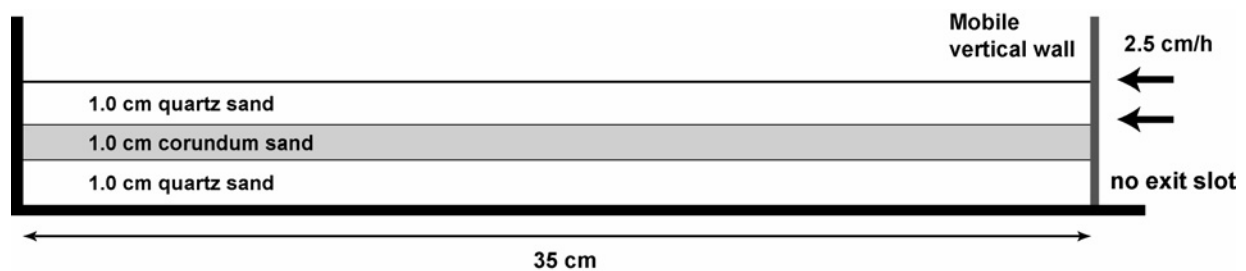


Fig. 9: Set-up of the brittle compressional wedge experiment 1B. All walls and the base are covered with Alkor foil.

4.2.2 Numerical model set-up

The experiment can be run at cm or km scale. If scaling up, please use 1 cm = 1 km and 2.5 cm/h = 2.5×10^{-7} m/h (6.944×10^{-11} m/s). The time step should be 3.6 s (cm-scale) or 3.6×10^{10} s (km-scale). The resolution of the models should be high enough so that an increasing resolution does not lead to different model results. Please report the number of solution nodes in the sand domain.

Similarly to experiment 1A, the velocity contrast between mobile wall and the base may be applied directly (method 1) or the velocity discontinuity may be smoothed (method 2). In the latter case, please linearly decrease the velocity from $v = 2.5$ cm/h over 2 mm to $v = 0$ at the base of the mobile wall. Specify which method you have used.

Please test whether your results are sensitive to a build-up phase for the driving velocity by experimenting with applying the full velocity at once or gradually building up the driving velocity in a number of iterations.

Please see ‘Numerical model materials’ (section 3.2) for additional instructions.

4.2.3 Required results

The experiment should be run until 10 cm of shortening. Analogue laboratories should run this experiment **twice**. Run an extra experiment (3 experiments total) if no Alkor foil is used on the sidewall to enhance visibility for PIV imaging (section 6). Numerical modellers should run this experiment for **3 to 5** different increasing resolutions, documenting that the resolution of the model is high enough. Provide all measurements for your optimum resolution, for the other resolutions, give points 1, 8, 9-12, 16, and 17 (see below). Please increase resolution with similar factors in horizontal and vertical directions.

Please provide:

1. Analogue and numerical models: Cross-sections at the following shortening increments: 0 cm, 0.2, 0.4, 0.5, 0.6, 0.8, 1.0, 1.5, 2.0, 2.5, 3.0 cm, 3.5, 4.0 etc to 10 cm. All analogue laboratories should report on the cross-sectional evolution as monitored from the side. Laboratories that have access to a scanner should in addition report the evolution for a cross-section through the middle of the domain (please specify the exact location of the cross-section). Numerical models should show the material field (to enable comparison with the analogue models). 3D numerical models should report the evolution of a cross-section through the middle of the domain (please specify exact location of the cross-section).
2. Analogue and numerical models: An animation of the cross-sectional evolution with each stage indicated.
3. Numerical models: show (1) strain-rate and (2) mean stress (pressure) at the same stages (point 1). Please use the scales (colour and intervals) in Fig. 7.
4. Analogue models and 3D numerical models: Surface views at the same stages (point 1).
5. Analogue models and 3D numerical models: Animation of surface views with stages indicated.
6. Analogue models: Surface photograph at 10.0 cm shortening of the basal domain over which the wall moved (including the wall itself).
7. Analogue models: Please cut the experiment at 10.0 cm of shortening and show (1) a section at 25% of the along-strike width, (2) a section in the middle – 2cm, (3) a section in the middle, (4) a section in the middle + 2 cm and (5) a section at 75% of the along-strike width. 3D numerical models: please show the same sections at 10 cm for comparison. Please include a surface view figure that indicates the exact location of the 5 cross-sections with distances along-strike of the mobile wall in cm.
8. Analogue and numerical models: Surface slope evolution at every 0.5 cm of shortening. Please measure through the valleys (following Stockmal and Beaumont, in press) as indicated in Fig. 10. Please provide figures of all your measurements (showing how you have drawn the surface slope).
9. Numerical models: Dissipation of energy at every 0.5 cm (in sand domain only):

$$\frac{1}{2} \int_A (\sigma \cdot \dot{\epsilon}) dA$$

Here A is area for 2D models and volume for 3D models. For 3D models, please provide also the 2D quantity through the middle of the domain (indicate the exact location of the section).

10. Numerical models: Gravitational rate of work at every 0.5 cm (in sand domain only):

$$\int_A (\rho g v_y) dA$$

Here A is area for 2D models and volume for 3D models. For 3D models, please provide also the 2D quantity through the middle of the domain (indicate the exact location of the section). ρ is density, g gravitational acceleration and v_y the vertical component of velocity.

11. Numerical models: root-mean-square (rms) velocity at every 0.5 cm (in sand domain only):

$$v_{rms} = \sqrt{\frac{1}{A} \iint (v_x^2 + v_y^2) dx dy}$$

The summation is over every solution node in the model domain and v is the velocity magnitude ($v^2 = v_x^2 + v_y^2$). For 3D models, please provide also the 2D quantity through the middle of the domain (indicate the exact location of the section).

12. Numerical models: Force applied at mobile wall at every 0.5 cm:

$$F = \int_h \sigma_{xx} dz$$

For 3D models, please also provide the equivalent 2D-model quantity for the middle of the domain (and indicate the exact location).

13. Analogue models analysed by X-ray computed tomography (CT): For those labs with a CT-scanner, measure the dip of the forward thrust in three different vertical sections at 25%, 50% and 75% of the length parallel to the mobile wall. In each section measure the dip of the forward thrusts and backthrusts as close to the moment of initiation as possible. An analogue shear zone is defined as formed when its trace can be seen at the surface (note that we do not require that it has already accumulated offset). Please measure the dip angle of each thrust at three heights: (1) at the base, (2) at 1.5 cm from the base, and (3) at 3 cm from the base (Fig. 11A). Report the amount of shortening at which the measurements are made. For those labs analysing through a glass sidewall use the same procedure for measuring the dips of thrusts at the moment of their initiation. In this case, please also measure the dip in the final cross-section at 10 cm of shortening which is cut through the middle of the model.
14. Numerical models: Please measure the dip angle of shear zones at the moment of their initiation. A numerical shear zone is defined as formed when it is visible in a finite strain plot and has just started to accumulate offset (which can still be very minor). Please measure the dip angle in an interval, which is 2 cm long measured along the shear zone and centred at 1.5 cm from the base of the model (Fig. 11B). Please specify whether forward or backthrusts are measured, report the amount of shortening at which the measurements are made and provide figures of all measurements.
15. Analogue models: Shear zone width at 10.0 cm of shortening. Please measure the width of all thrusts (forward and backward) at 1.5 cm from the base (Fig. 12). Measure perpendicular to the dip of the shear zone. Please provide the figures with your measurements indicated (may be drawn onto photographs).
16. Analogue and numerical models: Thrust spacing; Measure the horizontal distance from a forward thrust at the moment of its initiation to the previous forward thrust. Please measure near the surface as indicated in Fig. 13. Please provide the spacing, the shortening stage at which it is measured and figures of the measurements. For shear zone initiation see definitions in points 13 and 14.
17. Analogue and numerical models: Number of shear zones; Specify the amount of shortening at which a new shear zone forms (see points 13 and 14 for definition of a new shear zone).
18. Numerical models: Please document: resolution (number of solution nodes, type of element and number of elements horizontally x vertically (if applicable)), ψ , E , ν , whether smoothing is used at the velocity discontinuity, km-scale or cm-scale.

Please show cross-sectional evolution with ‘mobile wall’ moving **from right to the left**.

For numerical modellers: please scale down to the analogue experiments (cm-scale) if necessary. Please use 1 km = 1 cm, $10^{-11} \text{ s}^{-1} = 10^{-1} \text{ s}^{-1}$, 1 MPa = 10 Pa and $10^{24} \text{ Pa.s} = 10^9 \text{ Pa.s}$.

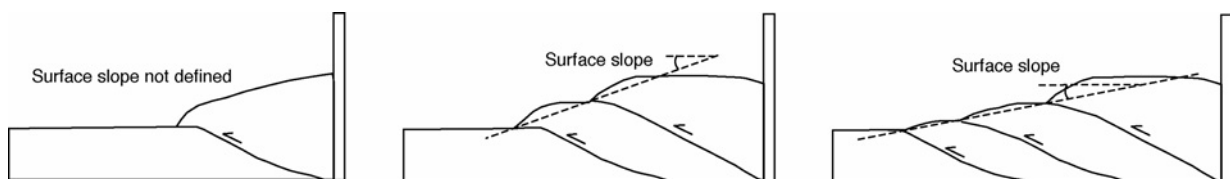
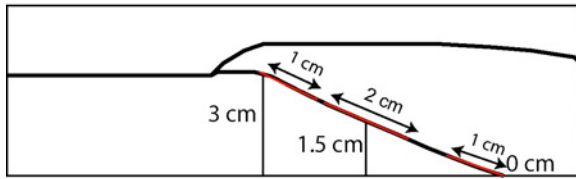


Fig. 10. Measurement of surface slope for experiments 1B and 2.

a) analogue experiments



b) numerical experiments

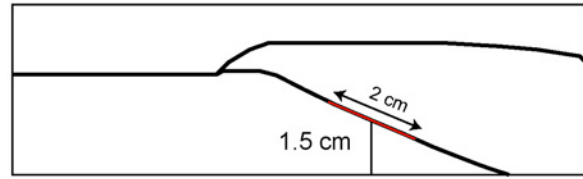


Fig. 11. Measurement of the dip angle of forward and backward thrusts for a) analogue experiments and b) numerical experiments

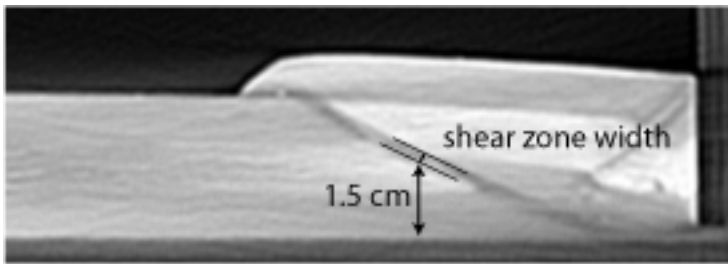


Fig. 12. Measurement of shear zone width in analogue experiments 1B and 2

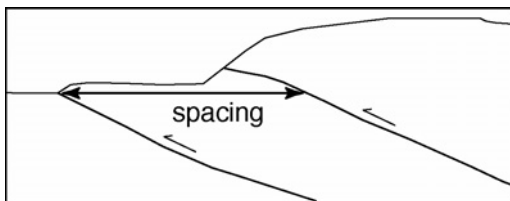


Fig. 13. Measurement of thrust spacing for experiments 1B and 2.

5 Experiment 2: Brittle shortening

The aim of this experiment is to examine shear zone evolution (dip, spacing, width) for a brittle material under compression (Fig. 14).

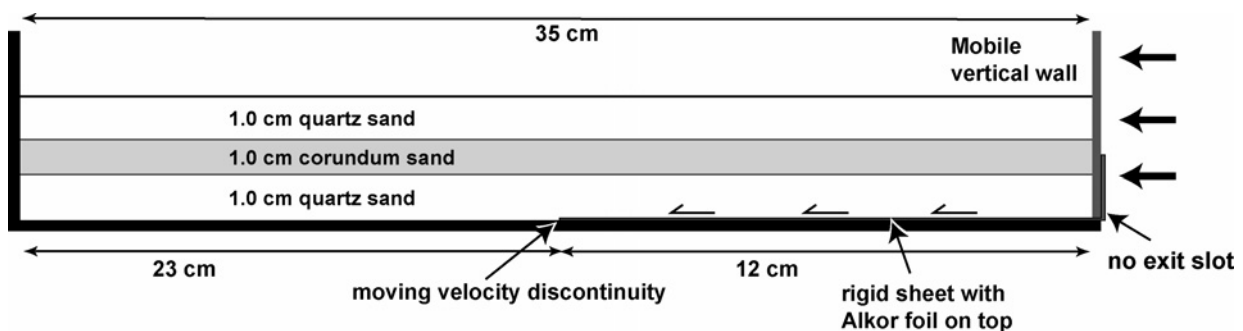


Fig. 14: Set-up of brittle shortening experiment.

5.1 Analogue model building procedure

The sheet should be a stiff carton of **1 mm** thick with Alkor foil on top. Please take care that no sand comes under the sheet (the tip of the sheet should not move up!). This is best achieved by slight upward (convex) pre-bending of the sheet, however, the sheet should remain horizontal. Make sure that the strike of the thrusts in surface view is parallel to the moving wall in the

middle of the domain.

Please see ‘Analogue model materials’ (section 3.1) for additional instructions.

5.2 Numerical model set-up

The tip of the sheet forms a velocity discontinuity. Similarly to experiments 1A and 1B, the velocity discontinuity may be applied directly for codes that can handle this (method 1). Otherwise, please linearly decrease the velocity from $v = 2.5 \text{ cm/h}$ at $x = 23 \text{ cm}$ over 2 mm to $v = 0$ at $x = 23.2 \text{ cm}$ (method 2). Specify which method you have used. The sheet should **not** be included in the model domain. The boundary condition representing the sheet is an applied velocity and boundary friction.

Please test whether your results are sensitive to a build-up phase for the driving velocity by experimenting with applying the full velocity at once or gradually building up the driving velocity in a number of iterations.

The experiment can be run at cm or km scale. If scaling up, use $1 \text{ cm} = 1 \text{ km}$ and $2.5 \text{ cm/h} = 2.5 \times 10^{-7} \text{ m/h}$ ($6.944 \times 10^{-11} \text{ m/s}$). The time step should be 3.6 s (cm-scale) or $3.6 \times 10^{10} \text{ s}$ (km-scale). The resolution of the models should be high enough so that an increasing resolution does not lead to different model results. Please report the number of solution nodes in the sand domain.

Please see ‘Numerical model materials’ (section 3.2) for additional instructions.

5.3 Parameters for quantification:

The experiment should be run until 10 cm of shortening. Analogue laboratories should run this experiment **twice**. Numerical models should run this experiment for **3 to 4** different resolutions. See Experiment 1B (section 4.2.3) for required results.

6 Application of high-resolution optical image correlation techniques to analogue experiments

The spatial and temporal pattern of deformation in analogue model experiments can be monitored in detail using high-resolution optical image correlation techniques (also known as Particle Imaging Velocimetry, PIV; e.g. Adam et al. (2005)). This technique makes it possible to establish the pattern of localized and distributed deformation much earlier than from visual inspection of the experiment. We therefore encourage participating labs to monitor the side views of their experiments with a digital camera.

The following details were kindly provided by David Boutelier and Christoph Schrank, who will carry out the PIV computations.

In order to optimize the PIV processing, the displacement increment in pixels between two successive images needs to be specified. A good image correlation is usually obtained if the interrogation window is 32×32 pixels or larger. In the PIV computations, a 32×32 pixels window size will be used and window displacement will be 8 pixels (75% overlap). The displacement increment corresponds physically to: $\Delta L = 8 \times R$, where R is the resolution, which

is the width of the field of view (in mm) divided by the number of pixels in the image width, thus: $R = W_{\text{mm}} / W_{\text{pix}}$ (mm/pix). To obtain the same displacement in pixel between two successive images, the time increment must change depending on the resolution of the image: $\Delta t = \Delta L / V = 8 \times R / V$ (where V is the imposed velocity in the experiments in mm/min). Table 2 gives the appropriate displacement increment (ΔL) in mm and the time interval (Δt) in minutes between successive pictures in the experiments for most common camera resolutions (capture size).

For example, if the field of view for the side pictures in the Experiment 1A (W_{mm}) is exactly 160 mm and the image width (largest dimension of capture size in landscape format) is 4000 pixels then R is 0.04 mm/pix, ΔL is 0.32 mm and Δt is 0.77 min. If your camera settings are not in Table 2, you should use the formulas above to compute the physical displacement increment and time interval. It is important that the field of view is approximately 16 cm in Experiment 1A and 36 cm in Experiments 1B and 2. The time increment may be chosen smaller than in Table 2, but the time when the displacement is about 8 pixels must be a multiple of the chosen Δt . For the previous example we had Δt of 46 s, but we can also obtain an image every $\Delta t/2$. For practical reasons the time interval may also be rounded to multiples of 60 or 30 seconds.

The digital photographs should be taken from the same viewpoint using a tripod. Variations in light conditions should be avoided as much as possible during the experiment. It is also important that the exposure time is properly chosen in order to get the maximum contrast within the model without under- (completely dark areas in grey scale) or over-exposure (completely white areas in grey scale). Sand grains on the outside of the sidewalls must be removed.

Capture size	Experiment 1A		Experiments 1B and 2	
	ΔL	Δt	ΔL	Δt
320 x 240	4	9.6	9	21.60
640 x 480	2	4.8	4.5	10.8
800 x 600	1.6	3.84	3.6	8.64
1024 x 768	1.25	3.0	2.81	6.75
1280 x 960	1.0	2.4	2.25	5.4
1536 x 1180	0.83	2.0	1.88	4.5
1600 x 1200	0.8	1.92	1.80	4.32
2048 x 1536	0.63	1.5	1.41	3.38
2240 x 1680	0.57	1.37	1.29	3.09
2560 x 1920	0.5	1.2	1.13	2.7
3032 x 2008	0.42	1.01	0.95	2.28
3072 x 2304	0.42	1.0	0.94	2.25
3264 x 2448	0.39	0.94	0.88	2.12
3888 x 2592	0.33	0.79	0.74	1.78
4000 x 3000	0.32	0.77	0.72	1.73
4368 x 2912	0.29	0.7	0.66	1.58
5188 x 3473	0.25	0.59	0.56	1.33

Table 2: Values of the displacement increment (ΔL) and time increment (Δt) between two successive images for most common capture sizes.

The exact value of the following parameters needs to be provided with the set of images:

- picture width, W_{mm} (in mm)
- resolution, R (in mm/pix)

- displacement increment (ΔL)
- time increment (Δt).

The images should be provided in tiff format, but jpegs could work as well provided the compression is kept at the minimum level. Unprocessed images can be uploaded on our ftp server: <ftp://geomod@camembert.geology.utoronto.ca> using the password *benchmark*. Create a subfolder in the folder /upload with the name of the group, the type of experiment and number of the experiment if several are performed (for example: Bern-1A-1 for the first experiment of the type 1A realised in Bern). The results of the PIV computations will be posted on the same ftp server in the folder /download.

7 Analogue sand and silicone properties benchmark

In the GeoMod2004 experiments several labs provided a quantification of their sand. It turned out that the range in, for example, the values for angle of internal friction and especially cohesion was large. The variation in these values may also be a function of the apparatus used, e.g. Hubbert-type shear box, Ring-shear tester. We therefore organise a benchmark of sands used in different analogue modelling laboratories. This is coordinated by Matthias Klinkmüller (University of Bern) and Matthias Rosenau (GFZ Potsdam). They use the Schulze Ring-Shear Tester at GFZ Potsdam (<http://www.dietmar-schulze.de/fre.html>). The computer-controlled Ring-Shear Tester RST-01.pc serves for determining the frictional properties of granular materials including the angle of internal friction for fault initiation (first peak strength), fault reactivation (second peak strength) and fault sliding (dynamic-stable strength). It can also be used to determine the boundary friction of granular material with respect to Alkor foil. For further details see Lohrmann et al. (2003) and Panien et al. (2006). The Schulze Ring-Shear Tester is certified and the apparatus and measuring procedure is described in a standard available from ASTM international (document nr. ASTM D6773-02; <http://www.astm.org>). The bulk modulus is measured with a uniaxial compression tester at GFZ Potsdam.

The following parameters are determined:

- Angle of internal friction at peak strength (fault initiation)
- Angle of internal friction at dynamic stable strength (fault sliding)
- Angle of internal friction at reactivation peak strength (fault reactivation)
- Apparent cohesion at peak strength, dynamic stable strength and reactivation peak strength
- Boundary friction of sand against Alkor foil
- Apparent cohesion of boundary friction
- Density
- Bulk modulus
- Dilation angle

Please send 7 kg of your sand to Matthias Rosenau at the address indicated below before **February 15th, 2008**. If your lab also uses coloured sand, then also send enough colouring material and describe in detail the procedure you use to colour the sand. In the latter case, the uncoloured sand will be tested first with the ring-shear tester. Subsequently, the sand will be coloured according to your colouring procedure and also measured with the ring-shear tester. Please respect the deadline, as the sand needs to be stored for several weeks in Potsdam under constant temperature and humidity.

Please send with your sand shipment a description of the characteristics of the sand (this is usually available from the distributor, but we would prefer your own measurements if possible):

- composition
- grain shape (microphotographs)
- grain size
- grain size distribution

In addition, there is also the possibility to measure the viscous materials that your lab uses with a Rheometer RC 20.1 at GFZ Potsdam. Send a 100 ml sample of your viscous material to the same address (indicated below). Deadline is also **February 15th, 2008**.

Material shipment address:

Matthias Rosenau,
 GFZ Potsdam,
 Geodynamiklabor Haus A14,
 Telegrafenberg,
 D-144473 Potsdam
 Germany.

8 Background: The GeoMod2004 Experiments

The GeoMod2004 experiments compared analogue and numerical results for a brittle shortening and a brittle-viscous extension experiment. Ten analogue modelling laboratories and eight numerical codes participated in this comparison. The aims of the experiments were to:

1. 'Benchmark' sandbox models,
2. Test the capability of different numerical methods to reproduce sandbox conditions,
3. Compare numerical and analogue results, in order to find the level of variability among results.

The results are published as (a pdf version of each article can be obtained from the first author):
 Schreurs, G., Buitter, S.J.H., Boutelier, D., Corti, G., Costa, E., Cruden, A., Daniel, J.-M., Hoth, S., Koyi, H., Kukowski, N., Lohrmann, J., Ravaglia, A., Schlische, R.W., Withjack, M.O., Yamada, Y., CavoZZi, C., DelVentisette, C., Elder Brady, J.A., Hoffmann-Rothe, A., Mengus, J.-M., Montanari, D., Nilforoushan F., Analogue benchmarks of shortening and extension experiments, in *Analogue and Numerical Modelling of Crustal-Scale Processes*, Geol Soc London Spec Publ 253, 1-27.

Buitter, S.J.H., Babeyko, A.Yu., Ellis, S., Gerya, T.V., Kaus, B.J.P., Kellner, A., Schreurs, G., Yamada, Y., The numerical sandbox: comparison of model results for a shortening and an extension experiment, in *Analogue and Numerical Modelling of Crustal-Scale Processes*, Geol Soc London Spec Publ 253, 29-64.

We learned that to first order, analogue and numerical results show a similar evolution with localisation of deformation onto shear zones and that different numerical solution methods successfully reproduce structures seen in the sandbox. However, a number of attention points arose:

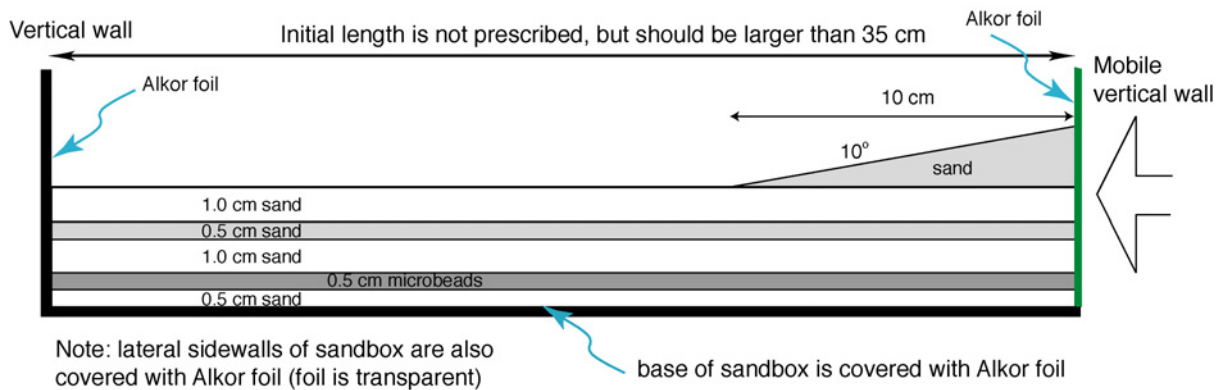
- 1) The level of variability among the results was rather large,
- 2) There were differences in detailed location, spacing, dip and evolution of shear zones,
- 3) The taper angle of the contractional brittle wedge in the shortening experiment was different between the various models,
- 4) It can be difficult to achieve an exact representation of analogue set-ups in a numerical model (e.g. boundary friction, velocity discontinuities).

These issues formed the motivation for the two new comparison experiments described in the beginning of this document.

In the GeoMod2004 experiments, each analogue laboratory used its own granular material and sandbox. The comparison experiments were therefore not a benchmark in the strictest sense. The silicone was the same for all laboratories (PDMS) and all walls and base of the modelling apparatus were covered with the same foil (Alkor foil).

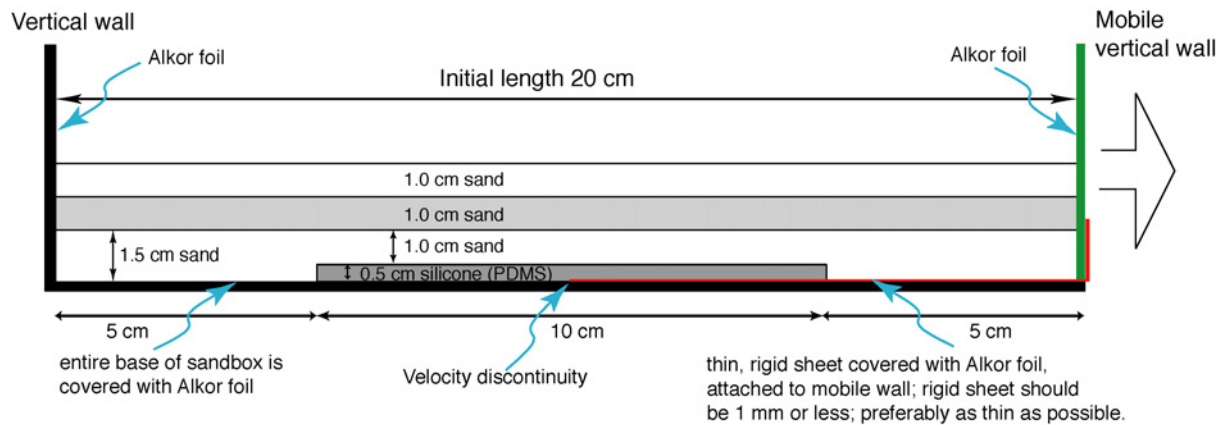
8.1 GeoMod2004 shortening experiment

The experiment was designed to test the influence of alternating strength layers on thrust wedge formation during contractional deformation. The model consists of a layer cake of competent and less competent brittle, granular materials: a 5 mm thick layer of sand (competent brittle material) at the base is overlain by a 5 mm thick layer of microbeads (incompetent brittle material), which on its turn is overlain by three layers of sand. A wedge of sand with a slope of 10° is added on top, next to the mobile wall and it extends 10 cm in length (as seen in cross-section).



8.2 GeoMod2004 extension experiment

The experiment tested the influence of a weak, basal viscous layer on basin formation in overlying brittle analogue materials. The base of the model is covered by a thin sheet, which is also covered with Alkor foil. The sheet extends 10 cm from the mobile wall and is attached to it (see drawing of set-up). The thin sheet with overlying foil at the base represents a velocity discontinuity. A 10 cm long and 5 mm thick slab of viscous silicone (polydimethyl-siloxane, PDMS SGM36, Weijermars, 1986) covers the central part of the model. Sand lies adjacent to and on top of the basal PDMS slab. The mobile wall (and the attached sheet) moves at a constant velocity of 2.5 cm/hour.



Note: lateral sidewalls should also be covered with Alkor foil (foil is transparent)

8.3 Material properties in GeoMod2004 numerical model experiments

The numerical material properties were prescribed, since the granular materials were different among the analogue modelling laboratories:

- Viscous silicone (PDMS): density 965 kg/m^3 , viscosity $5e4 \text{ Pa s}$
- Sand: density 1560 kg/m^3 , cohesion 10 Pa ; angle of internal friction 36° softening to 31° . The decrease in angle of internal friction is linear between total finite strain values of 0.5 and 1.0
- Microbeads: density 1480 kg/m^3 ; cohesion 10 Pa ; angle of internal friction 22° softening to 20° . The decrease in angle of internal friction is linear between total finite strain values of 0.5 and 1.0
- Sand on foil: angle of friction 19°
- The effects of elasticity in the granular materials are taken to be negligible

Acknowledgements

Figures 1, 2 and 5 were made by Matthias Klinkmüller. Matthias Rosenau measured the bulk modulus and dilation of the quartz and corundum sands. Matthias Klinkmüller measured the angle of internal friction, cohesion and boundary friction of the quartz and corundum sands. Taras Gerya run models to check the effect of dilation versus prescribed softening and Boris Kaus checked the effects of gradual loading of models in the initial step. We thank David Egholm, Taras Gerya, Susan Ellis, Matthias Rosenau, David Boutelier and Sandy Cruden for helpful discussions and lots of feedback.

References

- Adam, J., Urai, J., Wienecke, B., Oncken, O., Pfeiffer, K., Kukowski, N., Lohrmann, J., Hoth, S., Van der Zee, W., Schmatz, J., 2005. Shear zone formation and strain distribution in granular materials – new insights employing high-resolution optical image correlation. *Journal of Structural Geology* 27, 283-301.
- Dahlen, F.A., Suppe, J., Davis, D., 1984. Mechanics of fold-and-thrust belts and accretionary wedges: cohesive Coulomb theory. *Journal of Geophysical Research* 89, 10087–10101.
- Dahlen, F.A., Suppe, J., 1988. Mechanics, growth, and erosion of mountain belts. *Geological Society of America, Special Paper* 218, 161–178.
- Davis, D., Suppe, J., Dahlen, F.A., 1983. Mechanics of fold-and-thrust belts and accretionary wedges. *Journal of Geophysical Research* 88, 1153–1172.
- Jaeger, J.C., N.G.W. Cook and R.W. Zimmerman, 2007. *Fundamentals of rock mechanics*. Blackwell

- Publishing, 475 pp.
- Lohrmann, J., N. Kukowski, J. Adam and O. Oncken, 2003. The impact of analogue material properties on the geometry, kinematics, and dynamics of convergent sand wedges, *Journal of Structural Geology* 25, 1691-1771.
- Panien, M., G. Schreurs and A. Pfiffner, 2006. Mechanical behaviour of granular materials used in analogue modelling: insights from grain characterisation, ring-shear tests and analogue experiments, *Journal of Structural Geology* 28, 1710-1724.
- Roscoe, K.H., 1970. The influence of strain in soil mechanics. *Geotechnique* 20, 129-170.
- Schellart, W.P., 2000. Shear test results for cohesion and friction coefficients for different granular materials: scaling implications for their usage in analogue modelling. *Tectonophysics* 324, 1-16.
- Stockmal, G.S, Beaumont, C., Nguyen, M. and Lee, B. in press. Mechanics of thin-skinned thrust-and-fold belts: Insights from numerical models. In: J. Sears et al (Eds.): *Whence the mountains? Enquiries into the evolution of orogenic belts*, Geol. Soc. America Special Paper (Ray Price Volume).
- Turcotte, D.L. and G. Schubert, 2002. *Geodynamics*. Cambridge University Press, UK, 456 pp.
- Vardoulakis, I., 1980. Shear band inclination and shear modulus of sand in biaxial tests. *International Journal for Numerical and Analytical Methods in Geomechanics* 4, 103-119.
- Weijermars, R., 1986. Flow behaviour and physical chemistry of bouncing putties and related polymers in view of tectonic laboratory applications. *Tectonophysics* 124, 325-358.
- Zhao, W.-L., Davis, D.M., Dahlen, F.A., Suppe, J., 1986. Origin of convex accretionary wedges: evidence from Barbados. *Journal of Geophysical Research* 91, 10246–10258.